Insect Biochemistry and Molecular Biology 164 (2024) 104046

Contents lists available at ScienceDirect

Insect Biochemistry and Molecular Biology

journal homepage: www.elsevier.com/locate/ibmb

Evidence for a role of SNMP2 and antennal support cells in sensillum lymph clearance processes of moth pheromone-responsive sensilla

Sina Cassau, Jürgen Krieger *

Martin Luther University Halle-Wittenberg, Institute of Biology/Zoology, Department of Animal Physiology, 06120 Halle (Saale), Germany

ARTICLE INFO

Keywords:
Olfaction
Moth
Sensory neuron membrane protein
support cell
Long-chain fatty acids
Sensillum lymph

ABSTRACT

In insect antenna, following the activation of olfactory sensory neurons, odorant molecules are inactivated by enzymes in the sensillum lymph. How the inactivation products are cleared from the sensillum lymph is presently unknown. Here we studied the role of support cells (SCs) and the so-called sensory neuron membrane protein 2 (SNMP2), a member of the CD36 family of lipid transporters abundantly expressed in SCs, in sensillum lymph clearance processes in the moths *Heliothis virescens* and *Bombyx mori*. In these species, the sex pheromone components are inactivated to long-chain fatty acids. To approach a role of SNMP2 in the removal of such inactivation products, we analyzed the uptake of a fluorescent long-chain fatty acid analog into a newly generated HvirSNMP2-expressing cell line. We found an increased uptake of the analog into SNMP2-cells compared to control cells, which could be blocked by the CD36 protein inhibitor, SSO. Furthermore, analyses of sensilla from antenna treated with the fatty acid analog indicated that SNMP2-expressing SCs are able to take up fatty acids from the sensillum lymph. In addition, sensilla from SSO-pretreated antenna of *B. mori* showed reduced removal of the fluorescent analog from the sensillum lymph. Finally, we revealed that SSO pretreatment of male silkmoth antenna significantly prolonged the duration of the female pheromone-induced wing-fluttering behavior, possibly as a result of impaired lymph clearance processes. Together our findings in *H. virescens* and *B. mori* support a pivotal role of olfactory SCs in sensillum lymph maintenance processes and suggest an integral role of SNMP2 in the removal of lipophilic "waste products" such as fatty acids resulting from sex pheromone inactivation.

1. Introduction

The precise and sensitive detection of female-released sex pheromones by conspecific males is critical for the initiation of reproductive behaviors and mate finding in moths (Zhang et al., 2015; Stengl, 2010; Carde and Willis, 2008). Sex pheromones, like other volatile odorants, are detected by specialized olfactory sensory neurons (OSNs) on the antenna that extend their dendrites into hair-like cuticular protrusions, named sensilla (Zacharuk, 1985). The dendritic membranes of pheromone-sensitive OSNs contain narrowly tuned pheromone receptors (PRs) that transduce the chemical signal into an electrical response (Fleischer and Krieger, 2018; Stengl, 2010). Pheromone molecules enter the sensillum lumen through multiple cuticle pores (Keil, 1982, 1989; Steinbrecht, 1997). The lumen is filled with aqueous sensillum lymph that contains pheromone binding proteins supposed to transfer pheromone molecules through the lymph to their respective PRs. The protein and ionic composition of the sensillum lymph is maintained and regulated by so-called support cells (Leal, 2013; Thurm and Küppers, 1980; Schmidt and Benton, 2020), which border the sensillum lymph and moreover surround the OSNs at the bases of a sensillum, thus completing the olfactory unit (Sanes and Hildebrand, 1976; Steinbrecht and Gnatzy, 1984; Keil, 1989).

While the function of OSNs in the reception and discrimination of pheromones has thoroughly been investigated (Fleischer and Krieger, 2018; Zhang et al., 2015; Yew and Chung, 2017; Benton, 2022; Renou, 2014; Van der Goes van Naters, 2014), the specific role of the support cells in peripheral olfactory processes is largely unclear. A possible function of support cells has been suggested in governing sensillum lymph clearance processes by expressing proteins necessary for the elimination of "waste products" e. g. inactivated pheromone and odorant molecules (Vogt and Riddiford, 1981; Pelletier et al., 2023). In moths, such "waste products" are produced by different kinds of odorant degrading enzymes (ODEs) expressed in the antenna (Leal, 2013; Vogt et al., 2020), including aldehyde oxidases and dehydrogenases, which

* Corresponding author.
E-mail addresses: sina.cassau@zoologie.uni-halle.de (S. Cassau), juergen.krieger@zoologie.uni-halle.de (J. Krieger).

https://doi.org/10.1016/j.ibmb.2023.104046
Received 15 September 2023; Received in revised form 10 November 2023; Accepted 28 November 2023
Available online 2 December 2023

rapidly inactivate pheromones and thus prevent repeated stimulation of OSNs by the same molecule (Ishida and Leal, 2005; Vogt and Riddiford, 1981). For instance, in the major and minor sex pheromone components of the noctuid moth *Heliothis virescens,* Z11-Hexadecenal and Z9-Tetradecenal, the aldehyde moieties are transformed by ODEs into a carboxyl group resulting in the respective long-chain fatty acids of the same chain lengths (Tasayco and Prestwich, 1990). Similarly, in the silkmoth *Bombyx mori* ODEs transform the sex pheromone components, bombykol and bombykal in the sensillum lymph, to the long-chain fatty acid, E10, Z12-Hexadecadienoic acid (Fig. S1) (Pelletier et al., 2007; Rybczynski et al., 1990; Kasang and Weiss, 1974).

We previously identified a protein expressed in support cells potentially being involved in sensillum lymph clearance processes in moths, the so-called sensory neuron membrane protein type 2 (SNMP2) (Forstner et al., 2008; Cassau and Krieger, 2021; Blankenburg et al., 2019). SNMPs form an insect-specific clade of the large CD36 family of proteins (Robertson et al., 1999; Vogt et al., 2009; Nichols and Vogt, 2008) characterized by two transmembrane domains and a large extracellular region. Members of the CD36 family are described to act as lipid/lipoprotein receptors and transporters with CD36 itself facilitating the uptake of extracellular long-chain fatty acids (Pepino et al., 2014; Chen et al., 2022). While in moths as well as in flies the SNMP1 type is expressed in OSNs and implicated as a co-receptor for the sensitive and rapid detection of sex pheromones by PRs (Pregitzer et al., 2014; Benton et al., 2007; Jin et al., 2008), the SNMP2 type in moths is selectively expressed in support cells and its function is unexplored (Forstner et al., 2008; Blankenburg et al., 2019; Cassau and Krieger, 2021). By means of immunohistochemistry on antennal sections of *H. virescens,* we have localized HvirSNMP2 to the apical side of the support cells in olfactory sensilla adjacent to the sensillum lymph (Blankenburg et al., 2019). Due to its localization at the support cell/sensillum lymph interface and its membership to the CD36 protein receptor/transporter family, we hypothesize that SNMP2 in moths could potentially be involved in the removal of the lipophilic fatty acid pheromone inactivation products from the sensillum lymph. Therefore, in this study we aimed to assess the ability of the *H. virescens* SNMP2 protein to mediate the cellular uptake of long-chain fatty acids. Towards this goal, we generated a stable modified HEK293 cell line expressing HvirSNMP2 and tested SNMP2's ability to facilitate the uptake of a fluorescent long-chain fatty acid analog. Moreover, we analyzed if support cells in the antenna of *H. virescens* and another moth species, *B. mori*, are able to take up the fluorescent fatty acid analog from the sensillum lymph. Finally, we examined the consequences of an SNMP2-inhibitor on the cellular uptake of fatty acids into supports cells as well as the impact on the behavioral responses of male *B. mori* to female released sex pheromones. Overall, our data suggest a role of support cells and SNMP2 in sensillum lymph clearance processes that are of crucial importance for maintaining the functionality of pheromone-responsive sensilla in moths.

2. Materials and methods

2.1. Animals

Pupae of the tobacco budworm *Heliothis virescens* were kindly provided by Bayer CropScience AG, Monheim, Germany. Pupae of the silkmoth *Bombyx mori* were purchased from Laboratorio die Sericoltura, Centro die Ricerca Agricolutra e Ambiente (Padova, Italy). All animals were allowed to develop into adults and were used in experiments 0- to 4-days after eclosion.

2.2. Expression of HvirSNMP2 in Flp-In T-Rex293 cells

For the generation of a stable cell line allowing tetracycline-induced expression of HvirSNMP2 the components of the Flp-In-System (Thermo Fisher Scientific, Waltham, MA, USA) and a modified HEK 293 cell line (Flp-In T-REx293/G_α15) were used. Following protocols successfully applied previously (Grosse-Wilde et al., 2006; Pregitzer et al., 2014), the coding region of HvirSNMP2 (Acc. No. AM905328) were first PCR-amplified from vector containing the HvirSNMP2 cDNA (Forstner et al., 2008) using specific primers (HvirSNMP2: 5′- A TTT GCG GCC GCG ATG TTG GGC AAA CAC TCG AA-3′ and 5′- CCG GTC GAC CCA TCA ATT TCC TTT ATT AAC CTG -3′) and integrated into the pcDNA5/FRT/TO expression vector (Thermo Fisher Scientific). Subsequently Flp-In T-REx293/G_α15 cells were transfected with the HvirSNMP2/pcDNA5/FRT/TO construct using Lipofectamine™ 2000 Transfection Reagent (Thermo Fisher Scientific) according to the supplier's instructions. Briefly, 2 x 10^5 cells were seeded into single wells of a sterile 24-well cell culture plate (Greiner Bio-One, Frickenhausen, Germany) and transfected 24h later with 500 ng expression vector construct and 1 μL Lipofectamine 2000 reagent. 48h post transfection, cells were selected for SNMP2 genome integration using media supplemented with 100 mg/L hygromycin finally revealing the T-REx293/Gα15/SNMP2 cell line, named TREx/S2 cells in the following. TREx/S2 cells and control cells (T-REx293/Gα15/SNMP2), named TREx cells in the following, were cultured in T75 flasks (Sarstedt, Nümbrecht, Germany) using Dulbecco's Modified Eagle Medium (DMEM, Thermo Fisher Scientific) with 10% fetal bovine serum (Thermo Fisher Scientific) and supplemented with either 10 mg/L blasticidin, 200 mg/L geneticin in regular alternation. In the case of TREx/S2 cells, 100 mg/L hygromycin were regularly included. The heterologous expression of HvirSNMP2 in the TREx/S2 cells was induced by the addition of 5 μg/ml tetracycline to the cell culture medium.

2.3. RNA extraction and reverse transcription PCR

Total RNA was extracted from 90 to 95% confluent cells in T75 flasks pretreated with 5 μg/ml tetracycline 24h prior to using TRIzol reagent (Thermo Fisher Scientific) according to manufacturer protocol. Briefly, cells were suspended in 1 ml Trizol reagent, transferred into a 1.5 ml reaction tube and incubated for 5 min at room temperature. After adding 200 μL chloroform the samples were gently inverted for 30 s, followed by incubation for 2 min at room temperature and centrifugation for 15 min (12000 g at 4 °C). The clear upper aqueous layers were transferred to a fresh reaction tube, mixed with 500 μL isopropanol and kept overnight at −20 °C. After centrifugation for 30 min (12000 g, 4 °C), the supernatants were removed and the RNA pellets were washed with 1 ml 75% Ethanol. The samples were centrifuged again for 5 min (7500 g, 4 °C) and the supernatants removed. The RNA pellets were dried at room temperature and finally resuspended in 20 μL dH_2O. $PolyA^+$-RNA was isolated from total RNA using the Dynabeads mRNA purification kit (Thermo Fisher Scientific) following the protocol of the supplier and eluted in dH_2O. For first strand cDNA synthesis 150 ng of $polyA^+$-RNA, 1 μl 50 μM oligo(dT)20 primer (Thermo Fisher Scientific), 1 μl 10 mM 2-deoxynucleoside 5-triphosphate (dNTP) solution mix (New England Biolabs, Ipswich, MA, USA) and dH_2O were mixed in a total volume of 13 μL. After incubation for 5 min at 65 °C, 4 μl 5x SSIV Buffer (Thermo Fisher Scientific), 1 μl 100 mM 1,4-dithiothreitol (Thermo Fisher Scientific), 1 μl RNaseOut (Thermo Fisher Scientific), and 1 μl Superscript IV reverse transcriptase (Thermo Fisher Scientific) were added. Synthesis of cDNA was carried out at 52 °C for 10 min followed by 10 min at 80 °C. For PCR amplification of sequences coding for HvirSNMP2, the following primers were used: HvirSNMP2 5′-ATCAAA-GAGGACGATGTCCCGA-3′and 5′- CAGCTGTGGAATGTTGTTGATC-3'. PCR products were visualized using agarose gel electrophoresis and ethidium bromide staining.

2.4. SDS-PAGE and western blot

Cells were grown to a confluency of 80–90% in T75 flasks and induced by adding tetracycline to a final concentration of 5 μg/ml for 24h. Tetracycline addition was repeated 3h before collecting the cells for

protein analysis. Cells were washed off from the flask surface and transferred to a 2 ml reaction tube using 1.5 ml lysis buffer (50 mM Tris-HCl, 150 mM NaCl, 1 mM EDTA, pH 7.4) supplemented with 1% Triton X-100, 5% Glycerol and SigmaFAST protease inhibitor cocktail (Merck, Darmstadt, Germany; one tablet diluted in 100 ml of stock lysis buffer). After incubation for 3 min on an orbital shaker at room temperature, the samples were transferred to a fresh reaction tube, rotated for 30 min on an overhead shaker at 4 °C and subsequently centrifuged at 2000 g for 5 min at 4 °C. The supernatant was used for SDS-PAGE and Western Blot analysis. 20 μg of total protein of the supernatant were utilized per lane on a 12% SDS-gel. Two identically loaded gels were prepared in parallel and either stained with Coomassie blue, or electro blotted with a semi-dry apparatus onto a methanol-activated PVDF membrane (Carl Roth, Karlsruhe, Germany) soaked in transfer buffer (25 mM Tris, 192 mM glycine, 20% methanol) for 1h at 200 mA. After protein transfer, the membrane was incubated for 1h in TBST (100 mM Tris, 150 mM NaCl, pH 7.5 supplemented with 0.05% Tween 20) with 7% milk powder followed by treatment with the rabbit-anti-HvirSNMP2-ab (Blankenburg et al., 2019) diluted 1:500 in TBST with 3.5% milk powder overnight at 4 °C. Subsequently, the membrane was washed 3 times for 10 min with TBST, incubated in goat-anti-rabbit alkaline phosphatase (Thermo Fisher Scientific) diluted 1:10,000 in TBST with 3.5% milk powder for 1h at room temperature. After washing 3 times for 10 min in TBST and 2 times for 10 min in substrate buffer (100 mM Tris-HCl, 100 mM NaCl, 5 mM $MgCl_2$, pH 9.5) the membranes were incubated in 25 μg/ml nitro blue tetrazolium and 50 μg/ml 5-brom-4-chlor-3-indolyl phosphate in substrate buffer for 2h. The color reaction was stopped by incubating the membranes for 5 min in dH_2O.

2.5. Live cell imaging of fatty acid uptake

Cells (~30000 per well) were seeded onto 10-well CELLview™ Slides (Greiner Bio-One) 48h prior to the experiments and grown in 200 μl DMEM to a confluency of around 70–80%. Cells of different lines (TREx/S2, TREx) were seeded on the upper and the lower row of wells of the slides, respectively. 24h after seeding and at 5–6h before the experiments the cells were induced by adding 1 μl tetracycline solution (1 mg/ml). For live cell imaging, the cell-prepared slides were inserted into the microscope stage of a widefield fluorescence microscope DMi8 (Leica Microsystems, Wetzlar, Germany). Unless specified otherwise a 40× dry objective was used. The fatty acid uptake assay was conducted with one well at a time and started by carefully removing the growth medium and immediately adding 200 μL of working solution. The working solution consisted of a specific concentration of either a BODIPY™ FL C16- fluorescent fatty acid analog (BODIPY FL C16, Thermo Fisher Scientific, Stock solution: 10 mM in DMSO) or BODIPY™ 500/510 C_4, C_9 - fluorescent fatty acid analog (BODIPY C4C9, Thermo Fisher Scientific, Stock solution: 10 mM in DMSO), diluted in cell culture grade sterile filtered PBS pH 7.4 (Merck) and supplemented with 0.05% Trypan blue (Thermo Fisher Scientific) to quench extracellular BODIPY signals. For the SNMP2 inhibition experiments, cells were pretreated with 50 μM sulfo-N-succinimidyl oleate (SSO; Cayman Chemical, Ann Arbor, MI, USA) with 0.1% DMSO or only 0.1% DMSO in cell culture grade PBS for 60s prior to adding the working solution.

For monitoring the fluorescent fatty acid analog uptake into cells over time, images of the cells were captured in the transmitted light as well as the FITC fluorescence channels of the DMI8 microscope every 7s starting immediately after adding the working solution to the wells. 24 time points were recorded giving a total imaging time of 168 s. This protocol and duration turned out to be best to ensure full cell viability and exclude phototoxic effects in the experiments. For the recording the acquisition mode of the software Leica Application Suite X (LAS X, Leica Microsystems GmbH) was applied. The uptake of the fatty acid fluorescent analogs into single cells was evaluated by arbitrarily choosing cells as regions of interest (ROI) and tracing their outlines in the transmitted light channel using the Analysis function of LAS X. After selecting 25 cells per replicate in the transmitted light channel, the mean intensities of the labelled ROIs in the fluorescent FITC channel were extracted to calculate for each cell the relative change in fluorescent intensity over time by $(F_t\text{-}F_0)/F_0$. The mean (±SD) relative changes in fluorescent intensity ($\Delta F/F_0$) of TREx or TREx/S2 cells over time were calculated from all selected cells of at least four independent replicates using the LASx software.

2.6. Fluorescence immunohistochemistry (FIHC)

FIHC experiments were performed as described previously (Blankenburg et al., 2019). Antennae of adult *H. virescens* were fixed for 2 h at 4 °C in 4 % paraformaldehyde and 0.5 % glutaraldehyde in phosphate buffer (1.4 mM KH_2PO_4, 8 mM Na_2HPO_4, pH 7.4) followed by three washing steps for 10 min in phosphate buffered saline (PBS, 145 mM NaCl, 1.4 mM KH_2PO_4, 8 mM Na_2HPO_4, pH 7.1). Antennae were transferred into 10 % sucrose solution (in phosphate buffer) for 1 h at room temperature followed by 25 % sucrose solution (in phosphate buffer) over night at 8 °C. After embedding the antennae in O.C.T Tissue Tek freezing medium (Sakura Finetek Europe, Alphen aan den Rijn, The Netherlands) at −20 °C, 12 μm cryosections were prepared and subsequently thaw mounted onto Epredia SuperFrost Plus Adhesion microscope slides (Thermo Fisher Scientific). The sections were encircled with Liquid Blocker (Plano, Wetzlar, Germany) and then treated with PBS supplemented with 0.01 % Tween 20 for 5 min. Next, the sections were treated with 50 mM NH_4Cl (in PBS pH 7.1) for 5 min, PBS for 5 min and FIHC blocking solution (10 % normal goat serum, 0.5 % Triton X-100 in PBS pH 7.1), for 30 min at room temperature. Subsequently, the sections were incubated with rabbit-anti-HvirSNMP2 ab (1:200 in blocking solution) over night at 8 °C in a humid box, followed by washing the slides three times for 5 min with PBS and the incubation with goat-anti-rabbit AF488-conjugated secondary antibodies (1:1000) (Jackson ImmunoResearch, Ely, Great Britain), goat-anti-HRP Cy3 (1:400) (Jackson ImmunoResearch) and DAPI (1:1000, Thermo Fisher Scientific) diluted in PBS, for 1 h at room temperature. After washing the slides three times for 5 min with PBS, the sections were mounted in Mowiol (Merck; 20 g Mowiol 4–88, 2.4 g n-propyl-gallate, 40 ml glycerine, 80 ml PBS pH 7.1) and covered with a coverslip.

2.7. Whole mount in situ hybridization combined with immunohistochemistry

Whole mount fluorescent in situ hybridization (WM-FISH) was conducted as described earlier (Krieger et al., 2005) with a few modifications. For the experiments, 0.2 mL reaction tubes were used and all steps were incubated under constant rotation on an overhead shaker and at room temperature unless specified otherwise. Antennae of *B. mori* were prepared from cold anesthetized animals. The side branches were dissected from the main antennal stem and immediately transferred into 4% paraformaldehyde (in 100 mM $NaHCO_3$, pH 9.5). After incubation for 20–24h at 4 °C, the samples were washed for 1 min in PBS (pH 7.1), 10 min in 200 mM HCl and 2 min in PBS with 1% Triton X-100. The samples were then prehybridized at 55 °C in a hybridization oven (Jena Analytik, Jena, Germany) for at least 6h in whole mount hybridization solution [50% formamide, 5 × SSC (750 mM NaCl, 75 mM sodium citrate, pH 7.0), 1 × Denhardt's reagent (50 μg/mL yeast RNA, 1% Tween 20, 0.1% CHAPS, 5 mM EDTA) pH 8.0] followed by hybridization at 55 °C for 48–72 h in the same solution containing a digoxigenin labelled antisense RNA probe of the coding region of *B. mori* SNMP2 (Acc. No. XP_037870755). The DIG-labelled antisense riboprobe was generated from a BmorSNMP2 cDNA containing plasmid using an RNA transcription system (Merck).

Afterwards, the antennal samples were washed four times for 15 min in preheated 0.1 X SSC with 0.03% Triton X-100 at 60 °C in the hybridization oven and subsequently incubated in 1% blocking reagent (Akoya Biosciences, Marlborough, MA, USA) in TBS (100 mM Tris, 150

mM NaCl, pH 7.5) with 1% Triton X-100 over night at 4 °C. Samples were then treated with an anti-dig AP-conjugated antibody (Merck) diluted 1:500 in 1% blocking reagent in TBS for 48h at 4 °C. After washing five times for 10 min in TBS with 0.05% Tween 20 and one time for 5 min in 150 mM Tris-HCl pH 8.3, dig-labelled riboprobes were visualized by using the VECTOR RED alkaline phosphatase substrate kit (Vector Laboratories, Burlingame, CA, USA) as recommended by the manufacturer with components diluted in Tris-HCl (150 mM, pH 8.3) and substrate incubation for 5–7h at 4 °C. The samples were then washed with TBST three times for 10 min and treated with anti-HRP AF633 (Jackson ImmunoResearch) diluted 1:200 in TBST overnight at 4° for immuno-counterstaining of neurons. After washing the samples three times for 10 min with TBST and once for 5 min with H_2O, the antennal fragments were mounted in mowiol filled into the center of three layers of self-adhesive hole reinforcement rings (Herma GmbH, Filderstadt, Germany) placed on microscope slides and sealed with a coverslip.

2.8. Fatty acid uptake assay with antenna

The antennae of *H. virescens* and *B. mori* were carefully removed from the heads and placed into working solution (50 mM BODIPY FL C16 in PBS) for 1 h without submerging the base of the antenna. For *H. virescens,* the antennae were then briefly rinsed in PBS before being transferred into fixative solution (4% PFA in PBS) for 2h at 4 °C. The antennae were then washed three times for 10 min with PBS, embedded into O.C.T Tissue embedding medium, sectioned (12 μm) with a cryomicrotome and thaw mounted onto SuperFrost Adhesion microscope slides. After sectioning, the antennal sections were rinsed three times for 5 min with PBS, incubated in FIHC blocking solution for 30 min and then treated with anti-HRP Cy3 and DAPI for 1h. Sections were washed three times for 5 min in PBS, once for 5 min with H_2O and then mounted with mowiol and a cover slip. For *B. mori* antennae, the side branches were first dissected off of the main antennal branch and then transferred into the fixative solution overnight at 4 °C. Then the antennal fragments were rinsed twice with PBS for 10 min, briefly washed with water and transferring onto microscope slides with mowiol as described for the samples in WM-FISH. To test the effect of the SSO inhibitor on the antenna, the antenna were treated with an SSO solution (100 μM SSO, 0.4% DMSO in PBS pH 7.4) for 1 h at room temperature prior to the uptake assay with BODIPY FL C16. Afterwards, antenna were carefully removed at their bases and treated with the BODIPY FL C16 working solution as mentioned for *H. virescens*. Control experiments were performed with antenna treated in the same solution omitting SSO (0.4% DMSO in PBS pH 7.4).

2.9. Analysis of antennal samples by confocal microscopy

Sections from the FIHC experiments and whole mount preparations of the WM-FISH experiments, as well as the fatty acid uptake assays on moth antenna were analyzed on a LSM 880 confocal laser scanning microscope (Carl Zeiss Microscopy, Jena, Germany). Confocal image stacks of the fluorescence and transmitted-light channels were taken and used to make projections of optical planes applying the ZEN Black software (Carl Zeiss Microscopy). Pictures were not altered except for adjusting the brightness or contrast for a uniform tone within a single figure.

2.10. Behavioral experiments on Bombyx mori males

When exposed to females releasing sex pheromones, male silk moths respond by rapidly flapping their wings for some time, a behavior named the wing-fluttering response. To compare the response of untreated and SSO-Inhibitor-treated male *B. mori* to female released sex pheromones the duration of the flutter dance of the males was used as a measure. For this, 0–2 day old males were separately kept in plastic containers (11 cm × 7.5 cm x 4 cm). In the experiment, an adult female (0–3 day old) was held 10 cm above an individual male for 30 s eliciting an immediate male wing fluttering response. The total male response time was measured until the male stopped wing beating and remained stationary for more than 2 min. Afterwards, the male was placed head first until its thorax into a 2 ml reaction tube filled with 500 μL inhibitor solution (100 μM SSO with 0.4% DMSO in PBS pH 7.4), thus just its antenna and head were fully submerged in inhibitor solution. Control experiments were conducted with males treated in the same way with 0.4% DMSO in PBS. After treatment for 1h at room temperature, the males were placed back into their individual containers and left to dry for 15 min. Subsequently, the males were exposed again to females for 30 s and their wing flutter response was measured. The response durations of the males before and after their respective treatments were compared and analyzed for statistical differences using a paired T-test.

3. Results

3.1. SNMP2 mediates an increased cellular uptake of a fluorescent fatty acid analog

For functional investigations towards a possible involvement of the SNMP2 protein in the transport of lipophilic fatty acid compounds, we generated a stable cell line, termed TREx/S2 cells, carrying the HvirSNMP2 coding sequence. The transcription of the HvirSNMP2 gene in TREx/S2 cells after tetracycline induction was verified using reverse transcriptase PCR and HvirSNMP2 specific primers. Amplification of PCR products of the anticipated size were obtained with cDNA generated from TREx/S2 cells but not with cDNA from parental TREx cells (Fig. 1A). In order to test if gene expression also leads to the production of the SNMP2 protein, we performed Western blot analysis with total protein extracts of induced TREx and the TREx/S2 cells using an anti-HvirSNMP2 antibody (Fig. 1B). A clear band slightly above the predicted molecular weight of about 59 kDa was obtained only in the TREx/S2 cells. Since SNMP proteins display a number of glycosylation sites (Gomez-Diaz et al., 2016), we presume that post-translational modifications likely cause the HvirSNMP2 protein to run higher than the predicted molecular weight. Together, the results demonstrate successful expression of SNMP2 in the TREx/S2 line on both the mRNA and the protein level.

To determine if HvirSNMP2 can mediate an increased cellular uptake of lipophilic fatty acids, we incubated parental TREx cells and SNMP2-expressing TREx/S2 cells with a fluorophore-conjugated long-chain fatty acid analog, termed BODIPY FL C16. We first compared the fluorescent signals in both lines directly after the application of 10 μM BODIPY FL C16 (0 s) and at the end of the uptake assay (168 s later) (Fig. 1 C). No intrinsic fluorescence was observed in cells of either line directly after the addition of the fatty acid analog (0 s). In contrast, imaging of the same cells after 168 s, revealed only weak fluorescence signals in TREx cells whereas SNMP2-expressing TREx/S2 cells showed intense fluorescent labeling. This result shows that the amount of fluorescent fatty acid analog taken up by the TREx/S2 cells vastly differs from that of the TREx cells (Fig. 1 C).

In order to monitor the uptake of 10 μM BODIPY FL C16 over time, we performed live cell imaging experiments by measuring the fluorescence of individual cells in 7s increments over a period of 168 s after treatment (24 time points). From this we calculated for each time point the relative change of fluorescent intensity in relation to the initial fluorescence ($\Delta F/F_0$). The mean relative fluorescence changes (±SD) of cells determined from 5 independent experiments with 25 arbitrarily selected each are shown in Fig. 1 D. It is getting clear that the parental TREx cells show a steady but rather low increase in fluorescence intensity, i. e. an uptake of BODIPY FL C16. In comparison, the results for the SNMP2-expressing cells show a much higher and rapid uptake of the fluorescent fatty acid analog over the whole 168 s duration of the experiments (Fig. 1 D).

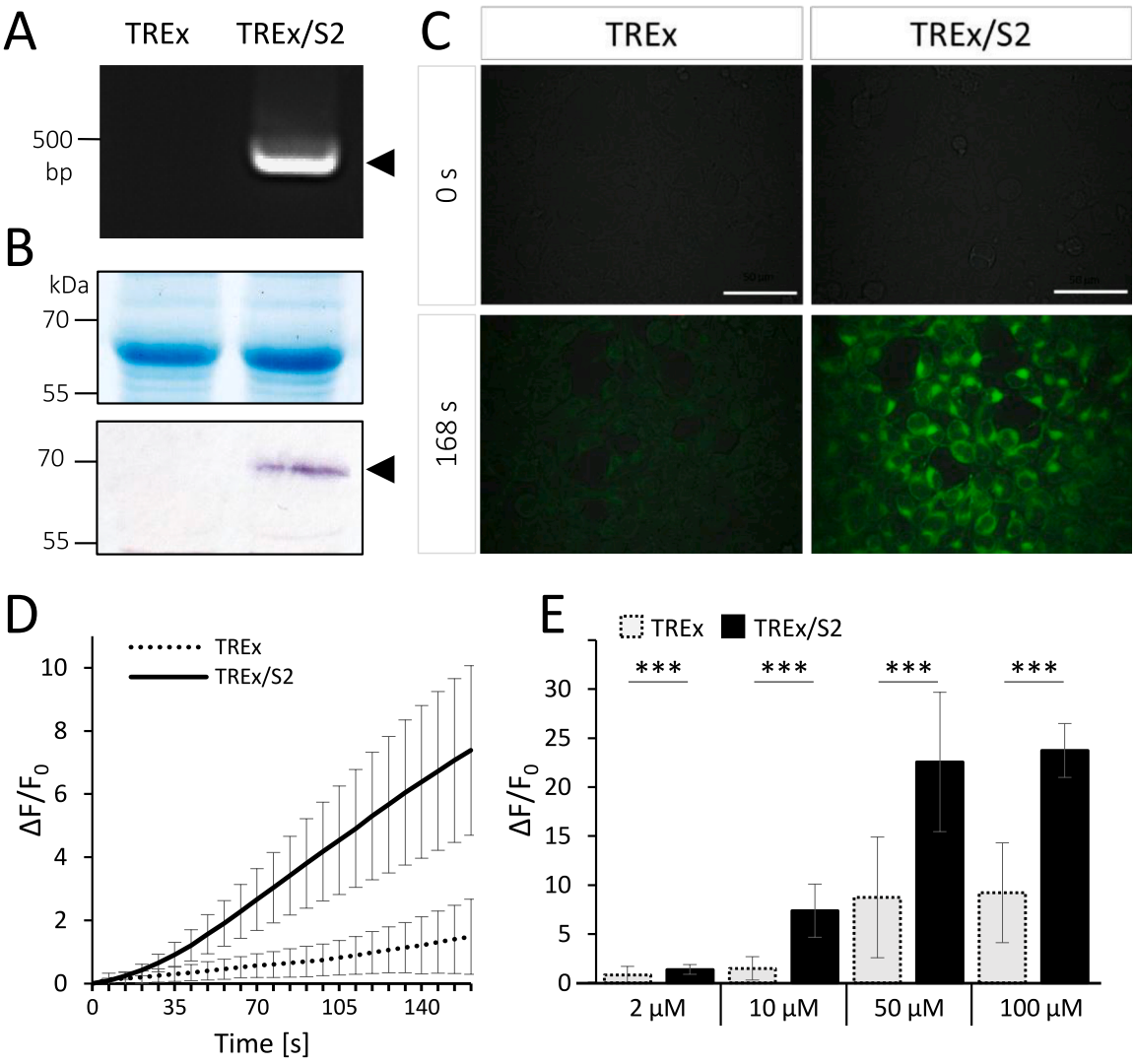

Fig. 1. SNMP2 mediates an increased cellular uptake of long-chain fatty acids. **A** SNMP2 gene expression in TREx/S2 as verified by RT-PCR with HvirSNMP2 specific primers. A band of the expected size (arrowhead) was only obtained with cDNA from TREx/S2 cells but not from the parental TREx cells. **B** SDS-PAGE and Western Blot analysis of total protein extracts from TREx and TREx/S2 cells. The upper panel shows all proteins of an SDS-PAGE stained with Coomassie blue. The lower panel shows the immunoblot using the anti-HvirSNMP2-ab that visualized a clear protein band in the TREx/S2 lane (arrowhead). **C** Uptake of BODIPY FL C16 (green) (10 µM) into TREx and TREx/S2 cells at 0s and at 168s after application of the fatty acid analog. Images were taken with a 63× immersion objective and processed with the Leica LASx software (scale bars = 50 µm). **D** live cell imaging measurements of the fatty acid uptake in TREx and TREx/S2 cells. Images were taken in 7s increments after the application of 10 µM BODIPY FL C16 using a 40× dry objective. The mean (±SD) relative changes in fluorescent intensity ($\Delta F/F_0$) in cells over time were calculated from five independent replicates with 25 randomly selected cells each using the LASx software. **E** relative changes of fluorescent intensity in TREx and TREx/S2 cells after 168s using different concentrations of BODIPY FL C16 (mean ± SD). Data were determined from five independent replicates with 20–25 cells each. Asterisks denote significant differences using an unpaired T-test (***$p < 0.001$).

We also tested parental TREx cells and the TREx/S2 cells with different concentrations of BODIPY FL C16 and compared the change in fluorescence intensity after 168 s (Fig. 1 E). We found a concentration dependent increase in fluorescence intensity in both cell lines. However, at all concentrations tested, a significantly higher fatty acid analog uptake was measured in the TREx/S2 cells compared to TREx cells. Overall, the results demonstrate that the presence of SNMP2 causes a rapid and increased cellular uptake of the long-chain fatty acid analog BODIPY FL C16 into TREx cells.

To approach the specificity of the BODIPY FL C16 uptake, further live cell imaging experiments were performed with another BODIPY fatty acid analog, BODIPY C4C9, where the position of the BODIPY fluorophore is shifted towards the middle of the molecule, closer to the fatty acid carboxyl group (Fig. S2). In these experiments, no differences in the uptake were observed between the TREx and the TREx/S2 cells (Fig. S3). These results denote some selectivity of SNMP2 in mediating the cellular uptake of lipophilic fatty acids.

3.2. *The CD36 inhibitor SSO impairs the SNMP2-mediated fatty acid uptake*

We next attempted to suppress the SNMP2-mediated uptake of long-chain fatty acids into TREx cells by applying a known CD36 protein inhibitor, sulfo-N-succinimidyl oleate (SSO). Therefore, we pretreated the TREx and TREx/S2 cells with 50 µM SSO for 1 min before testing the uptake of 10 µM BODIPY FL C16 by live cell imaging measurements. For TREx cells we found no difference in the time course and extent of the fatty acid analog uptake between the SSO pretreated cells (Fig. 2 A) and untreated cells (Fig. 1 D), indicating that SSO does not impair regular TREx cell functions. However, when analyzing TREx/S2 cells, we

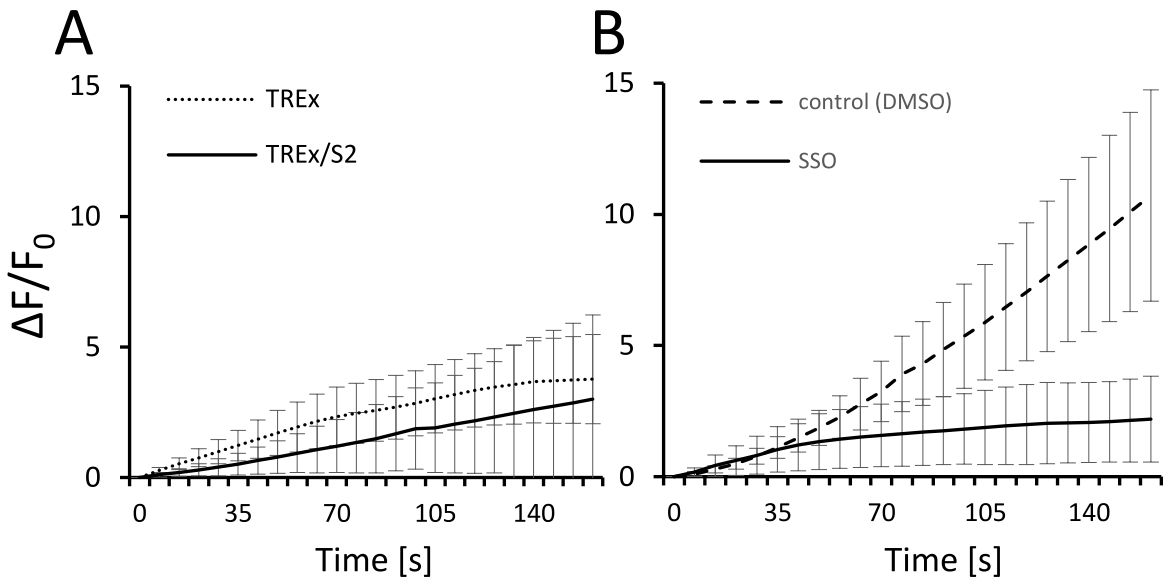

Fig. 2. SSO inhibits the SNMP2-mediated uptake of the long-chain fatty acid analog BODIPY FL C16. **A** Uptake of 10 μM BODIPY FL C16 in TREx and TREx/S2 cells after SSO pretreatment (50 μM SSO/0.1% DMSO). Live cell imaging measurements were performed in 7s increments over 168 s. The relative changes in fluorescent intensity ($\Delta F/F_0$) of the mean (±SD) cellular values calculated from four independent replicates with 25 randomly selected cells each. **B** TREx/S2 cells were either pretreated with 50 μM SSO/0.1% DMSO or only 0.1% DMSO (control) prior to live cell imaging of the BODIPY FL C16 uptake. $\Delta F/F_0$ changes represent the mean values (±SD) of cells calculated from six (SSO) and eight (control) independent replicates with 25 randomly selected cells each.

observed a clear reduction in fluorescence signal intensity in SSO-pretreated cells (Fig. 2A) compared to non-treated cells (Fig. 1 D), with the extent of the BODIPY FL C16 uptake in the SSO pretreated TREx/S2 cells now resembling the uptake in the parental TREx cells (Fig. 2 A). To ensure that the solvent (DMSO) used to solubilize SSO does not impact SNMP2 function, we performed additional control experiments with TREx/S2 cells preincubated with either the SSO working solution or the same solution without SSO (Fig. 2 B). This revealed no reduced uptake in TREx/S2 cells when SSO was omitted, demonstrating no effect of the DMSO solvent on SNMP2 function. Altogether, the experiments suggest that SSO inhibits SNMP2's function and in consequence attenuates the uptake of the lipophilic fatty acid analog BODIPY FL C16 into TREx/S2 cells.

3.3. Support cells of the H. virescens antenna express SNMP2 and can take up fatty acids from the sensillum lymph

We next tried to approach, whether an uptake of lipophilic fatty acids from the sensillum lymph may also exist in the antenna and whether SNMP2-expressing supports cells are involved. To investigate the ability of support cells to take up lipophilic fatty acids from the sensillum lymph, we incubated entire intact male *H. virescens* antennae in BODIPY FL C16 solution, allowing the compound to enter the sensillum lymph via pores in the sensillum's cuticle. After treatment, antennal sections were prepared and additionally treated with anti-HRP and DAPI to visualize neurons and nuclei, respectively.

The results of the antennal fatty acid uptake assays revealed intensive BODIPY FL C16 labeling of cells throughout the antennal segments as demonstrated by the horizontal section shown in Fig. 3 A. The BODIPY FL C16 labeling pattern was complementary to the neuronal staining that visualized OSNs (Fig. 3A–C), demonstrating that non-neuronal cells have specifically taken up the fatty acid analog. This is further evidenced by closer inspections of a longitudinal section, revealing that the BODIPY FL C16 signals are attributed to non-neuronal support cells, which directly border the bases of olfactory sensilla and are associated with OSNs that show no labeling by the fatty acid analog (Fig. 3 B and C, C'). Within the cells, the BODIPY FL C16 signals partly accumulated in a dot-like pattern (arrowheads in Fig. 3. C'). Control experiments with antenna incubated in a solution omitting the fluorescent fatty acid analog showed only the neuronal staining pattern and some cuticle's autofluorescence but no labelling in the green BODIPY fluorescence channel (Fig. S4).

In order to evaluate if the same cells that take up the fatty acid analog also express SNMP2, we set out to compare the support cell labeling pattern obtained in the BODIPY FL C16 uptake assay with the topography of the SNMP2-expressing support cells in the *H. virescens* antenna. Therefore, we performed FIHC with an anti-HvirSNMP2 specific antibody on antennal sections together with anti-HRP and DAPI counterstaining (Fig. 3 D - F'). Similar to the BODIPY FL C16 support cell labeling, the FIHC experiments exhibited the presence of SNMP2 in multiple, non-neuronal cells (Fig. 3 D and E). Moreover, exploring longitudinal sections shows that SNMP2 is localized in the support cells closely associated with OSNs at the bases of olfactory sensilla (Fig. 3 E and F). These results are in accordance with our previous FIHC and FISH experiments demonstrating broad SNMP2 expression in most if not all antennal support cells of *H. virescens* olfactory sensilla (Blankenburg et al., 2019; Forstner et al., 2008). Unfortunately, attempts to use the anti-SNMP2 antibody in BODIPY FL C16 uptake/SNMP2 co-labeling experiments were not successful. This was probably due to the extended protocol required for FIHC with anti-SNMP2-ab, leading to a loss of the BODIPY FL C16 signal from sections.

Overall, the support cell labelling pattern evoked by the anti-SNMP2 antibody clearly coincides with the pattern of BODIPY FL C16-positive cells revealed in the antennal fatty acid uptake assays. This strongly suggests that the SNMP2-expressing cells are the same support cells that are able to take up the fatty acid analog.

3.4. Fatty acid uptake and SNMP2-expression in support cells of the Bombyx mori antenna

To address the question if SNMP2-expressing support cells in other moths are also capable of taking up fatty acids from the sensillum lymph,

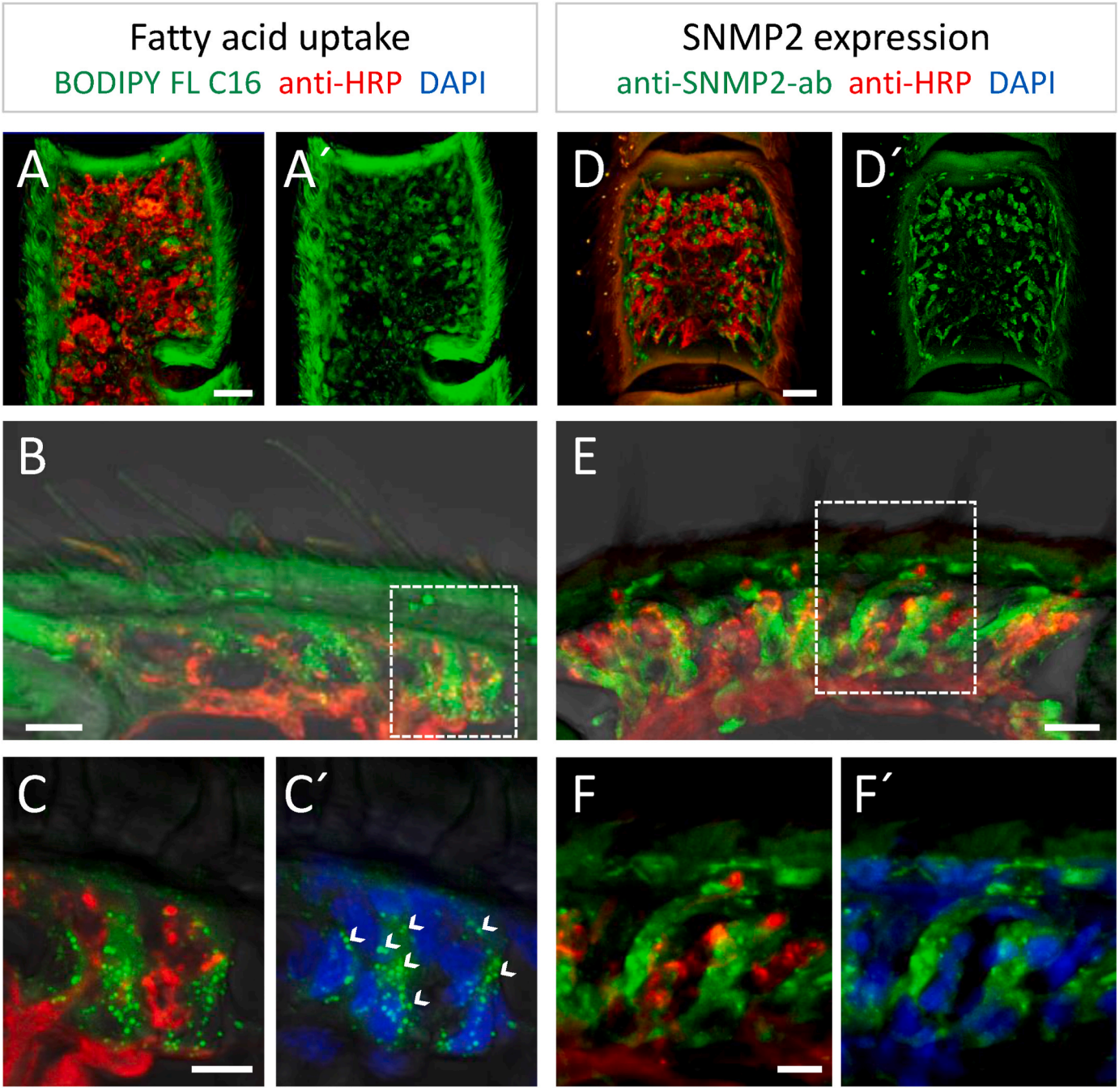

Fig. 3. Support cells of the antenna of *H. virescens* express SNMP2 and take up fatty acids from the sensillum lymph. Antennal sections were treated with anti-HRP to visualize OSNs (red) and DAPI to visualize nuclei (blue). **A-C**′ Sections of antenna that were incubated with the fatty acid analog BODIPY FL C16 (green). **A** and **A**′ Visualization of BODIPY FL C16-positive cells and neurons in a horizontal section. **B** Longitudinal section showing support cells that display BODIPY FL C16 signals and are associated with non-labelled OSNs underneath olfactory sensilla. **C** and **C**′ show a higher magnification of cells in the region boxed in B. Arrowheads indicate dot-like signals in support cells. **D-F**′ SNMP2-positive cells were visualized by FIHC using anti-HvirSNMP2-ab (green). **D** and **D**′ distribution of multiple non-neuronal SNMP2-positive cells and OSNs on a horizontal antennal section. **E** SNMP2 expression in support cells that are associated with OSNs underneath olfactory sensilla. **F** and **F**′ higher magnification of the boxed region shown in E. Images A, B, C, D, E, F: overlay of the red and green channels. A'and D' green channel. C'and F': overlay of the green and blue channels. Scale bars: A and D = 20 μm; B and E = 10 μm; C and F = 5 μm.

we analyzed the antenna of the silk moth *Bombyx mori.* Therefore, we first characterized the SNMP2-expressing cells in this species. In lack of a *B. mori* SNMP2-specific antibody we alternatively used fluorescence in situ hybridization (FISH) with a dig-labelled SNMP2 riboprobe combined with FIHC using the anti-HRP antibody to visualize the SNMP2-expressing cells and neurons, respectively.

Due to the distinctive morphology of the *B. mori* antenna, which has long sensilla on side branches that protrude out of a main trunk, sectioning of the antenna proved difficult. Therefore, we applied combined FISH/FIHC on whole mount samples of the antennal side branches. Using this method, we produced samples with well-preserved antennal tissue and sensilla structures, though we noted that in confocal LSM analysis the antennal cuticle emits strong autofluorescence depending on the optical plane being imaged (Fig. 4 A, asterisk).

In *B. mori*, all the trichoid and basiconic sensilla are located on one side of the antenna. Accordingly, we found anti-HRP labelled OSNs

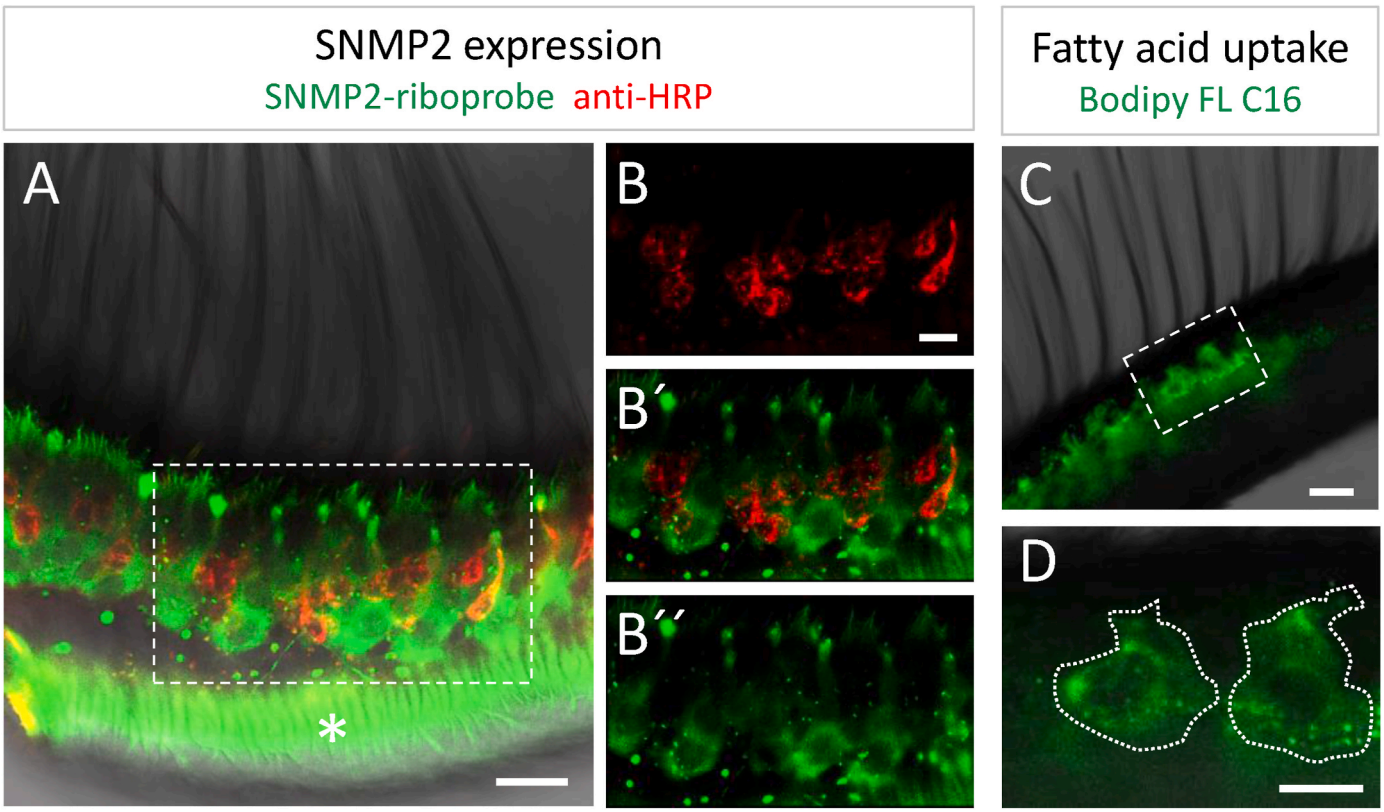

Fig. 4. Antennal support cells of *B. mori* express SNMP2 and can take up fatty acids from the sensillum lymph. **A-B''** Combined whole mount FISH and FIHC conducted on an antennal side branch utilizing an SNMP2-ribopobe (green) to visualize SNMP2 expression and anti-HRP (red) to visualize OSNs. **A** SNMP2-positive cells are situated beneath the olfactory sensilla. **B–B''** Show a higher magnification in different channels of the region boxed in A. **C-D** Antenna of *B. mori* treated with BODIPY FL C16 (green). **C** BODIPY FL C16-positive cells were detected underneath the olfactory sensilla. **D** higher magnification of the area boxed in C showing uptake of BODIPY FL C16 in support cells (encircled). The Asterisk (*) in A denotes autofluorescence of the cuticle. A and B': overlay of red and green channels. B: red channel. B'', C and D: green channel. Scale bars: A and C = 20 μm; B and D = 10 μm.

arranged below the antennal surface carrying the olfactory sensilla (Fig. 4 A and B). In addition, the SNMP2 riboprobe visualized numerous, strikingly large SNMP2-positive cells in the antenna that were closely associated with the OSNs (Fig. 4 A and B'). Typical for support cells, these cells show extension towards the base of the sensilla. In addition, the co-staining of OSNs and SNMP2-positive cells exemplifies the typical differences in the size and morphology of these cell types (Fig. 4 B'). Overall, the WM-FISH results elucidated a broad expression of SNMP2 in the morphologically distinct support cells in the antenna of *B. mori*.

We next tested if support cells of *B. mori* are also able to take up a fatty acid analog that enters a sensillum by incubating the antennae of males in a solution with BODIPY FL C16. In these experiments we found numerous cells displaying BODIPY FL C16 signals underneath the side of the antennal side branches harboring the majority of the olfactory sensilla (Fig. 4 C, supplementary). When analyzed at a higher magnification, it becomes apparent that BODIPY FL C16 signals, some of which appear as dot-like accumulations, are located in distinct and large cells, with a morphology typical for support cells and resembling the shape of the SNMP2-expressing cells. Together, our experiments with *B. mori* antenna revealed results similar to *H. virescens*, indicating the ability of support cells to take up fatty acids from the sensillum lymph, which, in terms of morphology and topography, correspond to SNMP2-expressing support cells.

3.5. SSO treatment of the antenna inhibits uptake of fatty acids from the lymph

To possibly link the observed BODIPY FL C16 uptake into antennal support cells to a role of SNMP2 in this process, we investigated if treatment of the antenna with the inhibitor SSO may impair the cellular uptake of the long-chain fatty acid analog from the sensillum lymph. Towards this goal we used the antenna of *B. mori* because it permits the analysis of whole mount preparations, which were regarded best suited for determining potential SSO inhibitor-induced changes of the BODIPY FL C16 uptake within antennal structures.

In control experiments antennal samples were pretreated for 1 h with 0.4% DMSO in PBS, which was used to dissolve SSO, before applying the fatty acid analog for 1 h. Analysis of the control samples visualized BODIPY FL C16-positive support cells, indicating that they retain their ability to take up fatty acids from the sensillum lumen upon solvent treatment (Fig. 5 A). In contrast, antenna subjected to SSO pretreatment (100 μM SSO, 0.4% DMSO in PBS) under otherwise identical conditions, showed diminished BODIPY FL C16 signals in the support cells (Fig. 5 B). Moreover, when analyzing the sensillum lumen, we noticed obvious differences in the luminal fluorescence signals between SSO-treated and control antenna (Fig. 5 C and D). Along the sensillum lumen of control antenna we rarely observed fluorescent signals, with occasional signals restricted to the base of the sensilla (Fig. 5 C). In contrast, in the SSO treated antenna, BODIPY FL C16 signals were regularly found localized along the entire length of the sensillum shafts (Fig. 5 D). Together our results demonstrate that SSO treatment of the antenna blocks the uptake of BODIPY FL C16 from the sensillum lymph into the support cells. Moreover, they indicate that this leads to an accumulation of the fatty acid analog in the sensillum lumen.

3.6. Effect of SSO treatment on pheromone-elicited behavior

In *B. mori*, the female-released sex pheromones, i. e. the unsaturated

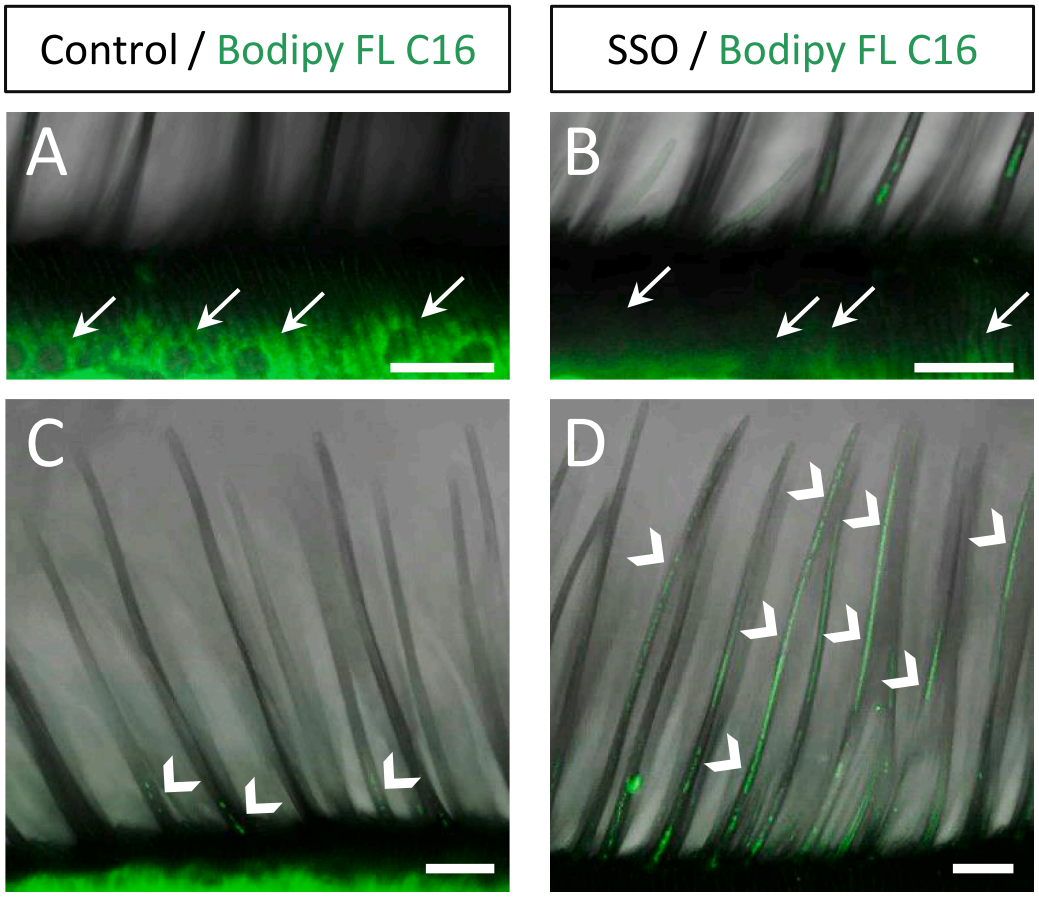

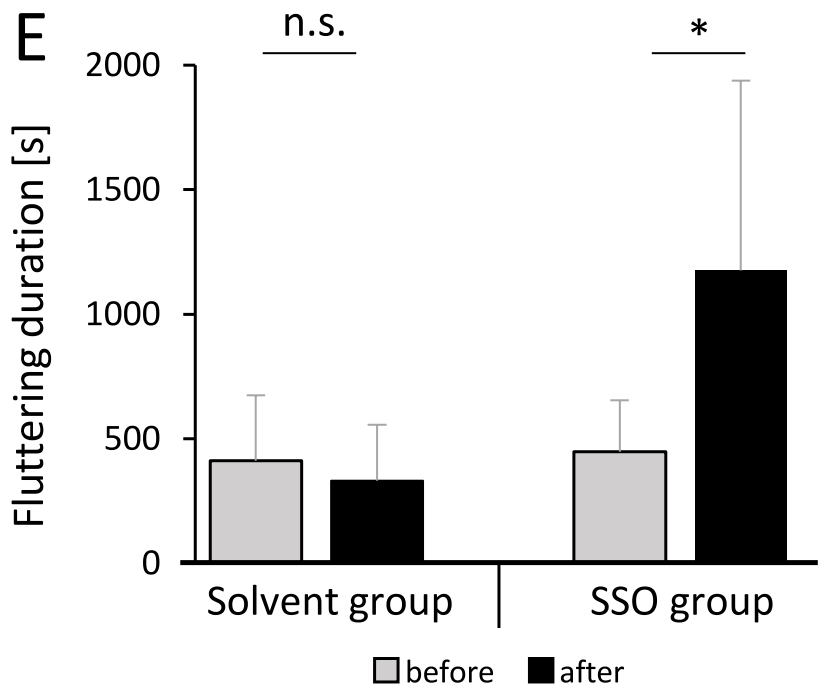

Fig. 5. SSO treatment of the *B. mori* antenna affects the uptake of fatty acids from the sensillum lymph and alters the behavioral response in males. Antenna were treated with either control (0.4% DMSO in PBPs) or inhibitor solutions (100 μM SSO, 0.4% DMSO in PBPs). **A-D** Antenna were incubated with the fatty acid analog BODIPY FL C16 (green) after treament. Scale bars = 20 μm. **A** Support cells (arrows) take up BODIPY FL C16 in control treatments. **B** Reduced uptake of BODIPY FL C16 into support cells after SSO treatment. **C** few BODIPY FL C16 signals (arrowheads) in the sensillum lumen in control treated antenna. **D** BODIPY FL C16 signals along the entire length of sensillum shafts in SSO treated antenna. **E** Wing fluttering duration of males (mean ± SD) after exposure to female pheromones before and after treatment with either solvent (n = 12) or SSO in solvent (n = 12). n.s. = not significant, **p = 0.0067 in a paired T-test.

long-chain alcohol and aldehyde Bombykol and Bombykal, respectively are inactivated to the corresponding long-chain fatty acids, which have to be rapidly removed from the sensillum lymph to prevent product inhibition of the inactivation process and, in consequence, accumulation of active sex pheromone in the lymph. Because we found SSO to impair the uptake of fatty acids from the lymph into support cells of *B. mori* we asked if SSO treatment of the antenna may possibly also alter the effective removal of sex pheromone inactivation products in males of *B. mori* and thus may lead to an altered behavioral response. We used the duration of the wing fluttering response as a measure to evaluate the impact of SSO on male pheromone-elicited behavior. First, we determined the duration of the wing-fluttering response of untreated individual males to female sex pheromone exposure. Subsequently, the intact antennae of individual males were incubated for 1 h in either PBS, 0.4 % DMSO (solvent-group) or 100 μM SSO in solvent (SSO-group). After allowing the antenna to dry for 15 min the exposure to females was repeated and the duration of the wing-fluttering response was determined again.

Prior to their respective treatments, the males of the SSO group (n = 12) and solvent group (n = 12) showed similar mean wing-fluttering response durations of 412 s (SD ± 263 s) and 448 s (SD ± 224 s), respectively. In males that were then treated with solvent, no significant differences in their wing-fluttering duration was found compared to before their treatment (Fig. 5 E), indicating that the solvent itself does not affect the duration of the male wing fluttering response. In contrast, in the SSO-group, we measured a significant difference between the duration of the wing-fluttering response before and after SSO treatment (Fig. 5 E). SSO treated males exhibited a prolonged wing-fluttering when presented to female releasing pheromones, with a mean duration of 1175 s (SD ± 764 s), which is more than twice the mean duration of the initial response. Overall, the experiments with *B. mori* show that SSO treatment of male antenna lead to altered behavioral responses to female sex pheromones, possibly due to disturbance of the proper removal of their fatty acid inactivation products.

4. Discussion

In this study we assessed a possible role of SNMP2 and support cells of insect olfactory sensilla in the elimination of lipophilic "waste products" from the sensillum lymph. In many moth species, such products result from the inactivation of female sex pheromones, representing long-chain unsaturated aliphatic alcohols or aldehydes, which are converted by ODEs in the sensillum lymph into the corresponding long-chain fatty acids following OSN activation (Tasayco and Prestwich, 1990; Pelletier et al., 2007; Rybczynski et al., 1990; Kasang and Weiss, 1974). The rapid pheromone inactivation and removal of their inactivation products from the sensillum lymph is considered to be essential for maintaining the functionality of the sensilla and thus the proper repetitive detection of pheromones (Vogt and Riddiford, 1981; Pelletier et al., 2023; Durand et al., 2011).

Our live cell imaging experiments with HvirSNMP2-expressing cells showed that the presence of SNMP2 mediates an increased and rapid cellular uptake of the fatty acid analog BODIPY FL C16 with increasing extracellular concentrations of the analog leading to an increased uptake into the cells. No increase in uptake was observed when testing the BODIPY C4C9 analog, indicating some ligand specificity of HvirSNMP2. Our findings for SNMP2 are reminiscent to functions of mammalian CD36 proteins, which facilitate the internalization of certain long-chain fatty acids into cells and accelerate the rate of fatty acid uptake (Koonen et al., 2005; Glatz and Luiken, 2018; Drover et al., 2008; Abumrad et al., 1993; Pepino et al., 2014; Glatz et al., 2022). Similarly, other insect-specific members of the CD36 family outside of the SNMP clade, namely NinaD and Santa Maria act in the uptake of lipids (carotenoids) (Wang et al., 2007; Kiefer et al., 2002; Giovannucci and Stephenson, 1999). Thus, a role of SNMP2s in the transport of lipophilic compounds across cell membranes is in line with the function attributed to various CD36 family members. In further support of functional similarities to the mammalian CD36 protein and of an SNMP2-mediated transport mechanism, we found that the CD36 inhibitor SSO abolished the BODIPY FL C16 uptake into SNMP2-expressing cells. In the mammalian CD36 protein, SSO binds to a distinct lysine in the apical part of the large protein ectodomain, which supposedly interacts with the carboxyl group of long-chain fatty acids, resulting in a reduction of the CD36-mediated fatty acid internalization (Pepino et al., 2014; Harmon and Abumrad, 1993; Kuda et al., 2013). Although it remains unknown how SSO impairs SNMP2's function, our data demonstrate that SSO is not just a potent inhibitor of mammalian CD36 proteins, but also of the insect-specific SNMP2 proteins.

In the antenna of *H. virescens* and *B. mori,* SNMP2 is exclusively expressed in the non-neuronal support cells found at the base of the sensilla. While in this study we focused on its possible role in the clearance of sex pheromone inactivation products, we are aware of SNMP2's broad expression in support cells of not only pheromone-sensitive sensilla but also of sensilla tuned to the reception of other behaviorally relevant odorants (Blankenburg et al., 2019; Gu et al., 2013; Sun et al., 2019). Therefore, it is conceivable that SNMP2 may also be involved in cleaning the sensillum lymph from inactivation products resulting from lipophilic general odorants or from lipophilic compounds that have entered a sensillum accidently. In experiments with *H. virescens* and *B. mori* we found that in SNMP2-expressing cells the same fatty acid analog, BODIPY FL C16 can be taken up, suggesting some overlapping ligand spectra of SNMP2 in different moth species. However, to clarify the selectivity and specificity of SNMP2 further investigations with a spectrum of various lipophilic ligand are necessary. Noteworthy, a previous study conducted on the moth *Lymantria dispar* has reported the presence high levels of long-chain fatty acids in the sensillum lymph (Nardella et al., 2015). This was suggested to facilitate pheromone partition in the lymph and pheromone binding to pheromone binding proteins. Therefore, in addition to pheromone clearance, the SNMP2 may also be involved in further processes i.e. homeostasis of the fatty acids that comprise the emulsion in the lymph.

Generally, members of the CD36 protein receptor/transporter family are multifunctional and have a broad ligand spectrum for various lipophilic molecules, including different long-chain fatty acids as well as other lipids derived from fatty acids (Silverstein and Febbraio, 2009; Martin et al., 2011; Abumrad and Goldberg, 2016; Zhao et al., 2021; Jimenez-Dalmaroni et al., 2009; Chen et al., 2022; Gomez-Diaz et al., 2016).

Based on our data, we suggest that SNMP2 proteins in support cells of insect antenna significantly contribute to the maintenance of the sensillum function by quickly removing undesired long-chain fatty acids from the sensillum lymph into support cells. In accordance with such a function, our previous detailed FIHC study on the antenna of *H. virescens* localized SNMP2 at the apical side of the support cells (Blankenburg et al., 2019), where microvilli structures largely increase the cellular surface of support cells and directly border the sensillum lymph (Keil, 1989; Gnatzy et al., 1984). Moreover, recent immunogold labelling experiments with locust antenna localized the SNMP2 protein in the microvilli-membranes of support cells (Cassau et al., 2022).

Microvilli structures are generally sites of high extensive exchange across membranes (Sharkova et al., 2023; Houdusse and Titus, 2021). Such an extensive exchange appears to also exist over the microvilli membranes of olfactory support cells. When treating intact antenna with the fluorescent fatty acid analog, we found that support cells of both *H. virescens* and *B. mori* were able to efficiently take up the compound from the sensillum lymph. This indicates that support cells of olfactory sensilla not only control sensillum lymph homeostasis by secreting proteins and ions (Thurm and Küppers, 1980), but also by absorbing molecules which could otherwise alter the composition of the sensillum lymph and impact the function of the olfactory unit. Interestingly, evidence for a clearance function of support cells was also provided by studying gustatory sensilla of the cockroach's maxillary palps infiltrated

with the fluorescent dye Lucifer yellow, where it was found that the support cells of these sensilla were able to take up and clear the substance from the sensillum lymph (Seidl, 1992). This may hint on a crucial role of support cells for sensillum lymph maintenance in olfactory and gustatory sensilla of insects.

In our antennal uptake assays with BODIPY FL C16, we regularly found fluorescent signals accumulating in a dot-like pattern within support cells of *H. virescens* and, albeit less pronounced, in support cells of *B. mori*. This may suggest that in olfactory support cells the absorbed lipophilic compounds end up in vesicles and subsequently in lipid droplets as described for the CD36-dependent uptake of free fatty acids in adipocytes, which appears to involve dynamic endocytosis processes leading to the formation of vesicles and lipid droplets (Hao et al., 2020).

We found that pretreatment of antenna with SSO led to a reduced uptake of BODIPY FL C16 from the sensillum lymph into support cells, resembling the reduced uptake observed upon SSO treatment of the SNMP2-expressing cell line. Notably, compared to sensilla of untreated antenna, the lumen of sensilla from SSO-incubated antenna showed strong fluorescent signals indicating that the lymph was still filled with significant amounts of the fatty acid analog. This finding further corroborates that SSO can interfere with the support cell's clearance of extracellular fatty acids from the sensillum lymph causing an accumulation of lipids in the perireceptor space. Whether this is a result of direct SSO binding to the SNMP2 expressed in the support cells needs to be investigated.

Since we observed that SSO impacts the proper function of sensilla with regard to the clearance of fatty acids, which are metabolites in the inactivation of female-released moth pheromones, we analyzed the possible consequences of an SSO inhibition on the pheromone-induced behavior of male *B. mori* moths. Males of this species react sensitively to the female's emitting pheromones with a typical fluttering of their wings, which we found considerably prolonged after SSO treatment. This suggests that SSO treatment has a substantial impact on the pheromone responsiveness of male moths by probably inhibiting the clearance of extracellular fatty acids derived from the inactivation of pheromones by ODEs. Worth mentioning, disrupting any part of the ODE activity also leads to prolonged olfactory responses (Chertemps et al., 2012; Fraichard et al., 2020), indicating that in general, the improper clearance of odorants can impact olfactory driven behavior.

Overall, our data suggest an important role of support cells in regulating the removal of lipophilic waste compounds from the sensillum lymph, thereby maintaining the proper function of the olfactory unit as a whole. In these processes SNMP2 may play an essential role in mediating the elimination of lipophilic fatty acids from the sensillum lymph such as the inactivation products of moth pheromones. In this way support cells and SNMP2 would ensure a rapid reset of the perireceptor environment in preparation to subsequent stimuli and might be of particularly relevance in moths to maintain the overall high temporal resolution of the pheromone detection system.

Author contributions

Sina Cassau: Conceptualization, Investigation, Methodology, Analysis and Interpretation of data, Visualization, Writing – original draft; Jürgen Krieger: Conceptualization, analysis and interpretation of data, Writing – review & editing.

Declaration of competing interest

The authors declare no conflict of interest.

Data availability

Data will be made available on request.

Acknowledgments

Doreen Sander is acknowledged for excellent technical assistance.

Appendix A. Supplementary data

Supplementary data to this article can be found online at https://doi.org/10.1016/j.ibmb.2023.104046.

References

Abumrad, N.A., El-Maghrabi, M.R., Amri, E.Z., Lopez, E., Grimaldi, P.A., 1993. Cloning of a rat adipocyte membrane protein implicated in binding or transport of long-chain fatty acids that is induced during preadipocyte differentiation. Homology with human CD36. J. Biol. Chem. 268, 17665–17668. https://doi.org/10.1016/S0021-9258(17)46753-6.

Abumrad, N.A., Goldberg, I.J., 2016. CD36 actions in the heart: lipids, calcium, inflammation, repair and more? Biochim. Biophys. Acta 1861, 1442–1449. https://doi.org/10.1016/j.bbalip.2016.03.015.

Benton, R., 2022. Drosophila olfaction: past, present and future. Proc. Biol. Sci. 289, 20222054 https://doi.org/10.1098/rspb.2022.2054.

Benton, R., Vannice, K.S., Vosshall, L.B., 2007. An essential role for a CD36-related receptor in pheromone detection in *Drosophila*. Nature 450, 289–293. https://doi.org/10.1038/nature06328.

Blankenburg, S., Cassau, S., Krieger, J., 2019. The expression patterns of SNMP1 and SNMP2 underline distinct functions of two CD36-related proteins in the olfactory system of the tobacco budworm *Heliothis virescens*. Cell Tissue Res. 378, 485–497. https://doi.org/10.1007/s00441-019-03066-y.

Carde, R.T., Willis, M.A., 2008. Navigational strategies used by insects to find distant, wind-borne sources of odor. J. Chem. Ecol. 34, 854–866. https://doi.org/10.1007/s10886-008-9484-5.

Cassau, S., Krieger, J., 2021. The role of SNMPs in insect olfaction. Cell Tissue Res. 383, 21–33. https://doi.org/10.1007/s00441-020-03336-0.

Cassau, S., Sander, D., Karcher, T., Laue, M., Hause, G., Breer, H., Krieger, J., 2022. The sensilla-specific expression and subcellular localization of SNMP1 and SNMP2 reveal novel insights into their roles in the antenna of the Desert Locust *Schistocerca gregaria*. Insects 13. https://doi.org/10.3390/insects13070579.

Chen, Y., Zhang, J., Cui, W., Silverstein, R.L., 2022. CD36, a signaling receptor and fatty acid transporter that regulates immune cell metabolism and fate. J. Exp. Med. 219 https://doi.org/10.1084/jem.20211314.

Chertemps, T., Francois, A., Durand, N., Rosell, G., Dekker, T., Lucas, P., Maibeche-Coisne, M., 2012. A carboxylesterase, Esterase-6, modulates sensory physiological and behavioral response dynamics to pheromone in *Drosophila*. BMC Biol. 10, 56. https://doi.org/10.1186/1741-7007-10-56.

Drover, V.A., Nguyen, D.V., Bastie, C.C., Darlington, Y.F., Abumrad, N.A., Pessin, J.E., London, E., Sahoo, D., Phillips, M.C., 2008. CD36 mediates both cellular uptake of very long chain fatty acids and their intestinal absorption in mice. J. Biol. Chem. 283, 13108–13115. https://doi.org/10.1074/jbc.M708086200.

Durand, N., Carot-Sans, G., Bozzolan, F., Rosell, G., Siaussat, D., Debernard, S., Chertemps, T., Maibeche-Coisne, M., 2011. Degradation of pheromone and plant volatile components by a same odorant-degrading enzyme in the cotton leafworm, *Spodoptera littoralis*. PLoS One 6, e29147. https://doi.org/10.1371/journal.pone.0029147.

Fleischer, J., Krieger, J., 2018. Insect pheromone receptors - key elements in sensing intraspecific chemical signals. Front. Cell. Neurosci. 12, 425. https://doi.org/10.3389/fncel.2018.00425.

Forstner, M., Gohl, T., Gondesen, I., Raming, K., Breer, H., Krieger, J., 2008. Differential expression of SNMP-1 and SNMP-2 proteins in pheromone-sensitive hairs of moths. Chem. Senses 33, 291–299. https://doi.org/10.1093/chemse/bjm087.

Fraichard, S., Legendre, A., Lucas, P., Chauvel, I., Faure, P., Neiers, F., Artur, Y., Briand, L., Ferveur, J.F., Heydel, J.M., 2020. Modulation of sex pheromone discrimination by a UDP-glycosyltransferase in *Drosophila melanogaster*. Genes 11. https://doi.org/10.3390/genes11030237.

Giovannucci, D.R., Stephenson, R.S., 1999. Identification and distribution of dietary precursors of the Drosophila visual pigment chromophore: analysis of carotenoids in wild type and ninaD mutants by HPLC. Vis. Res. 39, 219–229. https://doi.org/10.1016/S0042-6989(98)00184-9.

Glatz, J.F.C., Luiken, J., 2018. Dynamic role of the transmembrane glycoprotein CD36 (SR-B2) in cellular fatty acid uptake and utilization. J. Lipid Res. 59, 1084–1093. https://doi.org/10.1194/jlr.R082933.

Glatz, J.F.C., Nabben, M., Luiken, J., 2022. CD36 (SR-B2) as master regulator of cellular fatty acid homeostasis. Curr. Opin. Lipidol. 33, 103–111. https://doi.org/10.1097/MOL.0000000000000819.

Gnatzy, W., Mohren, W., Steinbrecht, R.A., 1984. Pheromone receptors in *Bombyx mori* and *Antheraea pernyi*. II. Morphometric analysis. Cell Tissue Res. 235, 35–42. https://doi.org/10.1007/BF00213720.

Gomez-Diaz, C., Bargeton, B., Abuin, L., Bukar, N., Reina, J.H., Bartoi, T., Graf, M., Ong, H., Ulbrich, M.H., Masson, J.F., Benton, R., 2016. A CD36 ectodomain mediates insect pheromone detection via a putative tunnelling mechanism. Nat. Commun. 7, 11866 https://doi.org/10.1038/ncomms11866.

Grosse-Wilde, E., Svatos, A., Krieger, J., 2006. A pheromone-binding protein mediates the bombykol-induced activation of a pheromone receptor *in vitro*. Chem. Senses 31, 547–555. https://doi.org/10.1093/chemse/bjj059.

Gu, S.H., Yang, R.N., Guo, M.B., Wang, G.R., Wu, K.M., Guo, Y.Y., Zhou, J.J., Zhang, Y.J., 2013. Molecular identification and differential expression of sensory neuron membrane proteins in the antennae of the black cutworm moth *Agrotis ipsilon*. J. Insect Physiol. 59, 430–443. https://doi.org/10.1016/j.jinsphys.2013.02.003.

Hao, J.W., Wang, J., Guo, H., Zhao, Y.Y., Sun, H.H., Li, Y.F., Lai, X.Y., Zhao, N., Wang, X., Xie, C., Hong, L., Huang, X., Wang, H.R., Li, C.B., Liang, B., Chen, S., Zhao, T.J., 2020. CD36 facilitates fatty acid uptake by dynamic palmitoylation-regulated endocytosis. Nat. Commun. 11, 4765. https://doi.org/10.1038/s41467-020-18565-8.

Harmon, C.M., Abumrad, N.A., 1993. Binding of sulfosuccinimidyl fatty acids to adipocyte membrane proteins: isolation and amino-terminal sequence of an 88-kD protein implicated in transport of long-chain fatty acids. J. Membr. Biol. 133, 43–49. https://doi.org/10.1007/BF00231876.

Houdusse, A., Titus, M.A., 2021. The many roles of myosins in filopodia, microvilli and stereocilia. Curr. Biol. 31, R586–R602. https://doi.org/10.1016/j.cub.2021.04.005.

Ishida, Y., Leal, W.S., 2005. Rapid inactivation of a moth pheromone. Proc. Natl. Acad. Sci. U. S. A. 102, 14075–14079.

Jimenez-Dalmaroni, M.J., Xiao, N., Corper, A.L., Verdino, P., Ainge, G.D., Larsen, D.S., Painter, G.F., Rudd, P.M., Dwek, R.A., Hoebe, K., Beutler, B., Wilson, I.A., 2009. Soluble CD36 ectodomain binds negatively charged diacylglycerol ligands and acts as a co-receptor for TLR2. PLoS One 4, e7411. https://doi.org/10.1371/journal.pone.0007411.

Jin, X., Ha, T.S., Smith, D.P., 2008. SNMP is a signaling component required for pheromone sensitivity in *Drosophila*. Proc. Natl. Acad. Sci. U. S. A. 105, 10996–11001. https://doi.org/10.1073/pnas.0803309105.

Kasang, G., Weiss, N., 1974. Thin-layer chromatographic analysis of radioactively labeled insect pheromones - metabolites of [bombykol-H-3. Journal of Chromatography 92, 401–417. https://doi.org/10.1016/S0021-9673(00)85751-9.

Keil, T.A., 1982. Contacts of pore tubules and sensory dendrites in antennal chemosensilla of a silkmoth: demonstration of a possible pathway for olfactory molecules. Tissue Cell 14, 451–462. https://doi.org/10.1016/0040-8166(82)90039-8.

Keil, T.A., 1989. Fine structure of the pheromone-sensitive sensilla on the antenna of the hawkmoth, *Manduca sexta*. Tissue Cell 21, 139–151. https://doi.org/10.1016/0040-8166(89)90028-1.

Kiefer, C., Sumser, E., Wernet, M.F., Von Lintig, J., 2002. A class B scavenger receptor mediates the cellular uptake of carotenoids in *Drosophila*. Proc Natl Acad Sci U S A 99, 10581–10586. https://doi.org/10.1073/pnas.162182899.

Koonen, D.P., Glatz, J.F., Bonen, A., Luiken, J.J., 2005. Long-chain fatty acid uptake and FAT/CD36 translocation in heart and skeletal muscle. Biochim. Biophys. Acta 1736, 163–180.

Krieger, J., Grosse-Wilde, E., Gohl, T., Breer, H., 2005. Candidate pheromone receptors of the silkmoth *Bombyx mori*. Eur. J. Neurosci. 21, 2167–2176. https://doi.org/10.1111/j.1460-9568.2005.04058.x.

Kuda, O., Pietka, T.A., Demianova, Z., Kudova, E., Cvacka, J., Kopecky, J., Abumrad, N. A., 2013. Sulfo-N-succinimidyl oleate (SSO) inhibits fatty acid uptake and signaling for intracellular calcium via binding CD36 lysine 164: SSO also inhibits oxidized low density lipoprotein uptake by macrophages. J. Biol. Chem. 288, 15547–15555. https://doi.org/10.1074/jbc.M113.473298.

Leal, W.S., 2013. Odorant reception in insects: roles of receptors, binding proteins, and degrading enzymes. Annu. Rev. Entomol. 58, 373–391. https://doi.org/10.1146/annurev-ento-120811-153635.

Martin, C., Chevrot, M., Poirier, H., Passilly-Degrace, P., Niot, I., Besnard, P., 2011. CD36 as a lipid sensor. Physiol. Behav. 105, 33–42. https://doi.org/10.1016/j.physbeh.2011.02.029.

Nardella, J., Terrado, M., Honson, N.S., Plettner, E., 2015. Endogenous fatty acids in olfactory hairs influence pheromone binding protein structure and function in *Lymantria dispar*. Arch. Biochem. Biophys. 579, 73–84. https://doi.org/10.1016/j.abb.2015.05.007.

Nichols, Z., Vogt, R.G., 2008. The SNMP/CD36 gene family in Diptera, Hymenoptera and Coleoptera: *Drosophila melanogaster, D. pseudoobscura, Anopheles gambiae, Aedes aegypti, Apis mellifera*, and *Tribolium castaneum*. Insect Biochem. Mol. Biol. 38, 398–415. https://doi.org/10.1016/j.ibmb.2007.11.003.

Pelletier, J., Bozzolan, F., Solvar, M., Francois, M.C., Jacquin-Joly, E., Maibeche-Coisne, M., 2007. Identification of candidate aldehyde oxidases from the silkworm *Bombyx mori* potentially involved in antennal pheromone degradation. Gene 404, 31–40. https://doi.org/10.1016/j.gene.2007.08.022.

Pelletier, J., Dawit, M., Ghaninia, M., Marois, E., Ignell, R., 2023. A mosquito-specific antennal protein is critical for the attraction to human odor in the malaria vector Anopheles gambiae. Insect Biochem. Mol. Biol. 159, 103988 https://doi.org/10.1016/j.ibmb.2023.103988.

Pepino, M.Y., Kuda, O., Samovski, D., Abumrad, N.A., 2014. Structure-function of CD36 and importance of fatty acid signal transduction in fat metabolism. Annu. Rev. Nutr. 34, 281–303. https://doi.org/10.1146/annurev-nutr-071812-161220.

Pregitzer, P., Greschista, M., Breer, H., Krieger, J., 2014. The sensory neurone membrane protein SNMP1 contributes to the sensitivity of a pheromone detection system. Insect Mol. Biol. 23, 733–742. https://doi.org/10.1111/imb.12119.

Renou, M., 2014. Pheromones and general odor perception in insects. In: Mucignat-Carettas, C. (Ed.), Neurobiology of Chemical Communication. CRC Press/Taylor & Francis, Boca Raton (FL).

Robertson, H.M., Martos, R., Sears, C.R., Todres, E.Z., Walden, K.K., Nardi, J.B., 1999. Diversity of odourant binding proteins revealed by an expressed sequence tag project on male *Manduca sexta* moth antennae. Insect Mol. Biol. 8, 501–518. https://doi.org/10.1046/j.1365-2583.1999.00146.x.

Rybczynski, R., Vogt, R.G., Lerner, M.R., 1990. Antennal-specific pheromone-degrading aldehyde oxidases from the moths *Antheraea polyphemus* and *Bombyx mori*. J. Biol. Chem. 265, 19712–19715. https://doi.org/10.1016/S0021-9258(17)45430-5.

Sanes, J.R., Hildebrand, J.G., 1976. Structure and development of antennae in a moth, *Manduca sexta*. Dev. Biol. 51, 280–299. https://doi.org/10.1016/0012-1606(76)90144-5.

Schmidt, H.R., Benton, R., 2020. Molecular mechanisms of olfactory detection in insects: beyond receptors. Open Biol 10, 200252. https://doi.org/10.1098/rsob.200252.

Seidl, S., 1992. Structure and function of the thecogen cell in contact chemosensitive sensilla of periplaneta-Americana L (Blattodea, Blattidae). Int. J. Insect Morphol. Embryol. 21, 235–250. https://doi.org/10.1016/0020-7322(92)90019-J.

Sharkova, M., Chow, E., Erickson, T., Hocking, J.C., 2023. The morphological and functional diversity of apical microvilli. J. Anat. 242, 327–353. https://doi.org/10.1111/joa.13781.

Silverstein, R.L., Febbraio, M., 2009. CD36, a scavenger receptor involved in immunity, metabolism, angiogenesis, and behavior. Sci. Signal. 2, 1–8. https://doi.org/10.1126/scisignal.272re3.

Steinbrecht, R.A., 1997. Pore structures in insect olfactory sensilla: a review of data and concepts. Int. J. Insect Morphol. Embryol. 26, 229–245. https://doi.org/10.1016/S0020-7322(97)00024-X.

Steinbrecht, R.A., Gnatzy, W., 1984. Pheromone receptors in *Bombyx mori* and *Antheraea pernyi*. I. Reconstruction of the cellular organization of the sensilla trichodea. Cell Tissue Res. 235, 25–34. https://doi.org/10.1007/bf00213719.

Stengl, M., 2010. Pheromone transduction in moths. Front. Cell. Neurosci. 4, 133. https://doi.org/10.3389/fncel.2010.00133.

Sun, L., Wang, Q., Zhang, Y., Yan, Y., Guo, H., Xiao, Q., Zhang, Y., 2019. Expression patterns and colocalization of two sensory neurone membrane proteins in *Ectropis obliqua* Prout, a geometrid moth pest that uses Type-II sex pheromones. Insect Mol. Biol. 28, 342–354. https://doi.org/10.1111/imb.12555.

Tasayco, M.L., Prestwich, G.D., 1990. Aldehyde-oxidizing enzymes in an adult moth: in vitro study of aldehyde metabolism in *Heliothis virescens*. Arch. Biochem. Biophys. 278, 444–451. https://doi.org/10.1016/0003-9861(90)90283-5.

Thurm, U., Küppers, J., 1980. Epithelial physiology of insect sensilla. In: Locke, M., Smiths, D.S. (Eds.), Insect Biology in the Future. Academic Press, New York, pp. 735–763.

Van Der Goes Van Naters, W., 2014. Drosophila pheromones: from reception to perception. In: Mucignat-Carettas, C. (Ed.), Neurobiology of Chemical Communication. CRC Press/Taylor & Francis, Boca Raton (FL).

Vogt, R.G., Miller, N.E., Litvack, R., Fandino, R.A., Sparks, J., Staples, J., Friedman, R., Dickens, J.C., 2009. The insect SNMP gene family. Insect Biochem. Mol. Biol. 39, 448–456. https://doi.org/10.1016/j.ibmb.2009.03.007.

Vogt, R.G., Riddiford, L.M., 1981. Pheromone binding and inactivation by moth antennae. Nature 293, 161–163. https://doi.org/10.1038/293161a0.

Vogt, R.G., Sparks, J.T., Fandino, R.A., Ashourian, K.T., 2020. Reflections on antennal proteins: the evolution of pheromone binding proteins. In: Blomquist, G., Vogts, R.G. (Eds.), Diversity of Pheromone Degrading Enzymes; and the Distribution and Behavioral Roles of SNMPs. Insect Pheromone Biochemistry and Molecular Biology. Elsevier Academic Press, London.

Wang, T., Jiao, Y., Montell, C., 2007. Dissection of the pathway required for generation of vitamin A and for *Drosophila* phototransduction. J. Cell Biol. 177, 305–316. https://doi.org/10.1083/jcb.200610081.

Yew, J.Y., Chung, H., 2017. Drosophila as a holistic model for insect pheromone signaling and processing. Curr Opin Insect Sci 24, 15–20. https://doi.org/10.1016/j.cois.2017.09.003.

Zacharuk, 1985. In: Kerkutt, G.A., Gilberts, L.S. (Eds.), Antenna and Sensilla. Comprehensive Insect Physiology, Biochemistry and Pharmacology. Pergammon, Oxford, pp. 1–69.

Zhang, J., Walker, W.B., Wang, G., 2015. Pheromone reception in moths: from molecules to behaviors. Prog. Mol. Biol. Transl. Sci. 130, 109–128. https://doi.org/10.1016/bs.pmbts.2014.11.005.

Zhao, L., Li, Y., Ding, Q., Li, Y., Chen, Y., Ruan, X.Z., 2021. CD36 senses dietary lipids and regulates lipids homeostasis in the intestine. Front. Physiol. 12, 669279 https://doi.org/10.3389/fphys.2021.669279.